Impact of surface coating and environmental conditions on the fate and transport of silver nanoparticles in the aquatic environment

Ellis, Laura-Jayne; Valsami-Jones, Eugenia; Baalousha, Mohammed ; Lead, Jamie

DOI:
10.1016/j.scitotenv.2016.05.199

Document Version
Peer reviewed version

Citation for published version (Harvard):
Ellis, L-J, Valsami-Jones, E, Baalousha, M & Lead, J 2016, 'Impact of surface coating and environmental conditions on the fate and transport of silver nanoparticles in the aquatic environment', *Science of the Total Environment*, vol. 568, pp. 95-106. https://doi.org/10.1016/j.scitotenv.2016.05.199

Impact of Surface Coating and Environmental Conditions on the Fate and Transport of Silver Nanoparticles in the Aquatic Environment

Laura-Jayne. A. Ellis[1], Eugenia Valsami-Jones[1], Jamie. R. Lead[1,2*] , and Mohammed Baalousha[2*],

[1]*School of Geography, Earth and Environmental Sciences, University of Birmingham, Edgbaston, Birmingham, B15 2TT, U.K.*

[2]*Center for Environmental Nanoscience and Risk (CENR), Department of Environmental Health Sciences, Arnold School of Public Health, University of South Carolina, Columbia, 29208, USA.*

*Corresponding Authors: Jlead@mailbox.sc.edu and Mbaalous@mailbox.sc.edu

Content **Page**

Highlights

- Aquatic microcosms were used to study the transport and behavior of AgNPs in model low and high ionic strength waters.
- Surface coating and solution chemistry has a major impact on AgNP stability.
- UV-Visible spectrophotometry provided important information on the aggregation and migration of the AgNPs.
- Experiments showed that PVP-coated AgNPs migrate via diffusion in all conditions, whereas citrate-coated AgNPs follow both sedimentation and diffusion dependent upon the aquatic environments.

Abstract

The role of surface coating (polyvinylpyrrolidone (PVP) and citrate) and water chemistry on the fate and behaviour of AgNPs in aquatic microcosms is reported in this study. The migration and transformation of the AgNPs was examined in low (ultrapure water- UPW) and high ionic strength (moderately hard water – MHW) preparations, and in the presence of modelled natural organic matter (NOM) of Suwannee River Fulvic Acid (SRFA). The migration and fate of the AgNPs in the microcosms was validated using a sedimentation-diffusion model and the aggregation behaviour was monitored by UV-visible spectrometry (UV-vis). Dissolved and particulate Ag concentrations (% Ag) were analyzed by ultrafiltration methods. Imaging of the AgNPs was captured using transmission electron microscopy (TEM).

Results indicate that PVP-coated AgNPs (PVP-AgNPs) remained stable for 28 days with similarly distributed concentrations of the PVP-AgNPs throughout the columns in each of the water conditions after approximately 96 hours (4 days). The sedimentation-diffusion model confirmed PVP-AgNP stability in each condition, by showing diffusion dominated transport by using the original unaltered AgNP sizes to fit the parameters. In comparison, citrate AgNPs were largely unstable in the more complex water preparations (MHW). In MHW, aggregation dominated behavior followed by sedimentation/dissolution controlled transport was observed. The addition of SRFA to MHW resulted in small stabilizing effects, to the citrate coated AgNPs, producing smaller sized AgNPs (TEM) and mixed sedimentation and diffusion migration compared the studies absent of SRFA. The results suggest that

surface coating and solution chemistry has a major impact on AgNP stability, furthermore the corresponding modeling will support the experimental understanding of the overall fate of AgNPs in the environment.

1 Introduction

Silver nanoparticles (AgNPs) are commercially exploited for their antibacterial and other properties(Benn and Westerhoff 2008),(Piccinno, Gottschalk et al. 2012). Although there are uncertainties, some studies have found AgNPs to be potentially toxic(Fabrega, Luoma et al. 2011) with adverse effects on biota(Navarro, Baun et al. 2008). Due to their extensive use in consumer products, it is also inevitable that AgNPs will enter the aquatic environment(Benn and Westerhoff 2008). Environmental fate and exposure models indicate that the predicted environmental concentrations (PECs) of AgNPs in surface waters will be in the range of ng to µg L^{-1} (Gottschalk, Sun et al. 2013). The quantities of NPs and rates of release will influence environmental concentrations, and be heavily impacted by their environmental behavior and transformations(Dale, Casman et al. 2015). The fate of the NPs is determined by key processes such as dissolution, aggregation, sedimentation, deposition, and sulfidation[(Lowry, Gregory et al. 2012),(Peijnenburg, Baalousha et al. 2015)]. These processes are largely influenced by the chemical complexity of the aquatic system such as ionic strength, pH and natural organic matter (NOM), and also the nature of the NPs(Peijnenburg, Baalousha et al. 2015). Deposition of AgNPs onto solid surfaces will reduce the migration of the AgNPs in suspension and influence their long term fate in the environment (Bae et al, 2013). Aggregation will increase particle size, reduce surface area and influence dissolution(Hotze, Phenrat et al. 2010) resulting in settling and sedimentation dominated migration which is a likely pathway for AgNPs. However, it has also been suggested that AgNPs can be modified by NOM leading to prolonged persistence in surface waters(La Farre, Pérez et al. 2008). Furthermore, capping agents are designed to increase colloidal stability of the AgNPs by reducing the surface energy(Ju-Nam and Lead 2008), which prevent interactions with the surrounding environment and avoid NP-NP interactions reducing aggregation rates(Kvitek, Panáček et al. 2008).

For charge stabilized-AgNPs, low ionic strength and high concentrations of NOM minimize homoaggregation(Chinnapongse, MacCuspie et al. 2011), whereas high ionic strength usually causes significant aggregation, even in the presence of high NOM concentrations most likely as a result of bridging mechanisms by divalent cations[(Baalousha, Nur et al. 2013),(Chen and Elimelech 2007)]. However, sterically-stabilized AgNPs are generally more stable than charge-stabilized NPs and are less likely to undergo

aggregation and sedimentation, even at high ionic strengths[Baalousha, Arkill et al. 2015),(Hitchman, Smith et al. 2013)] and often less prone to dissolution.

The aim of the current study is to produce a model to validate the environmental fate and migration behavior of AgNPs by investigating their behavior in static water 'microcosms'. In particular, this paper reports the impact of water chemistry and AgNP surface coating (citrate and PVP) on the fate of AgNPs over a period of 28 days. The concentration and aggregation behavior of AgNPs were measured by atomic absorption spectroscopy (AAS) and UV-visible spectrophotometry (UV-vis). The measured Ag concentrations were fitted using a diffusion-sedimentation model[Hinderliter, Minard et al. 2010),(Socolofsky and Jirka 2005)] to illustrate the dominant fate processes (*e.g.* aggregation and sedimentation, or diffusion) controlling the fate of Ag NPs in a range of synthetic waters from pure water to moderately hard water spiked with fulvic acid as a surrogate of natural organic matter.

2 Materials and Methods

2.1 Materials

Commercially available chemicals and solvents were purchased from Sigma-Aldrich (Dorset, UK) and were of analytical reagent grade. Ultra pure water (UPW) with a maximum resistivity of 18.2 $M\Omega cm^{-1}$ was used throughout the experiments. Suwannee River fulvic acid (SRFA) was purchased from the International Humic Substances Society (IHSS, St. Paul, MN, USA). Atomic force microscopy (AFM) cantilevers were purchased from Park systems corp, Suwon, Korea and used for AFM analysis. More information about the materials used in this experiment is provided in the supporting information (Table SI.1).

2.2 Synthesis and Characterization of AgNPs

Citrate-coated silver nanoparticles (cit-AgNPs) were synthesized by following a published methodology(Cumberland and Lead 2009) using reagent grade chemicals shown in table SI.1. Briefly, a 100 mL (0.25 mM) silver nitrate ($AgNO_3$) solution was mixed with a 100 mL (0.25 mL) sodium citrate solution, followed by addition of 6 mL (0.25 mM) sodium borohydride ($NaBH_4$). The mixture was then heated at 100 ^oC for 2 hours, while stirring vigorously. The resulting suspension was then refrigerated overnight at 4^oC and purification was carried out using a Millipore stirred cell ultrafiltration (1 kDa) system under nitrogen gas. PVP-AgNP suspensions(Tejamaya, Römer et al. 2012) were prepared by cooling a solution of (2 mM) $NaBH_4$ and PVP (M_w 10000, Sigma Aldrich) to 4^oC. $AgNO_3$ (1 mM) was added to the suspension dropwise with vigorous stirring. The suspensions were refrigerated overnight at 4^oC. Ultrafiltration using a Millipore stirred ultrafiltration cell with a cellulose membrane of 1 kDa (purchased from Sigma) under nitrogen (N_2) gas at approx 14 PSI was performed to remove Ag ions.

A multi-method approach was used to characterize the AgNPs, both ‘as prepared AgNPs’ and samples withdrawn from the microcosm. Dynamic light scattering (DLS), was used to measure hydrodynamic size using a Malvern Nanosizer 5000. Particle core size was measured by transmission electron microscopy (TEM, particle equivalent circular diameter) and AFM (particle height).

Samples were prepared by drop casting methods by depositing a 20 µL drop of AgNP suspension on a 300 mesh carbon-coated copper TEM grid (Agar Scientific, UK) for TEM analysis, and a freshly cleaved mica sheet for AFM analysis. The AgNP suspension drop was left for approximately 30 minutes to allow the NPs to adhere to the carbon membrane coating the TEM grid and the mica sheets for AFM. Both the TEM grids and the mica sheets were then rinsed with UPW to remove excess water, avoid NP aggregation and salt crystallization(Baalousha and Lead 2012).

All TEM analyses were performed using a JEOL 1200EX 100kv Max system or a Tecnai F20 Field Emission gun (FEG) TEM coupled with an X-ray energy dispersion spectroscopy (EDS) detector from Oxford Instruments. For each sample, a minimum of 100 particles from different randomly selected sample areas of multiple grids, were used to calculate the size and shape measurements using Digital Micrograph software (Gatan Inc, Pleasanton, CA, USA). The measured sizes were then classified into intervals of 0.5 nm to construct particle size distribution histograms.

All AFM analyses were performed using an XE-100 AFM (Park systems Corp., Suwon, Korea). The measurements were carried out in true non-contact mode using a Silicon cantilever with a typical spring constant of 42 N m^{-1} (PPP-NCHR, Park systems Corp., Suwon, Korea). All scans were performed at ambient conditions, which have been shown to produce accurate sizing, despite loss of most, but not all water[(Baalousha and Lead 2013),(Balnois and Wilkinson 2002)]. Images were recorded in topography mode with a pixel size resolution of 256 × 256 and a scan rate of 0.5-1.0 Hz. Height measurements of the AgNPs were made using the transect analysis using the XEI data processing and analysis software of the microscope (Park Systems Corp., Suwon, Korea). For each sample, a minimum of 100 height measurements were performed, which are sufficient to produce a representative particle size distribution(Baalousha and Lead 2012). The measured heights were then classified into intervals of 0.5 nm to construct particle size distribution histograms.

Total silver (Ag) concentrations were measured by flame atomic absorption spectroscopy (FAAS) using a Perkin Elmer instrument AAnalyst 300, with an air-acetylene mixture. Limits of FAAS instrumentation detection were devised by running a set of blanks (ultrapure water) which were measured at 2 ± 2 µg L^{-1} and a set of standards to determine a concentration of 50 µg L^{-1}. The concentrations of AgNPs in the purified NP suspensions were 11 mg L^{-1} and 20 mg L^{-1} for the cit- and PVP-AgNPs, respectively.

The surface plasmon resonance (SPR) of AgNP suspensions was measured using a Jenway 8300 double beam UV-visible spectrometer (UV-vis) over the wavelength range of 300-800 nm, with the use of suitable controls (UPW and MHW water). A 10 cm long path length cuvette was used to collect spectra. Full details of AgNP properties are provided in Table 1 and Figures S1-S9 in the Supporting Information.

Table 1: Properties of the 'as-prepared' AgNPs obtained using a multi-Method Characterisation approach

Technique	Citrate AgNPs	PVP AgNPs
Particle core size measured by TEM (nm)	11 ± 3	11 ± 2 nm
Particle height measured by AFM (nm)	12 ± 3	11 ± 3
z-average hydrodynamic diameter measured by DLS (nm)	21 ± 2	20 ± 2
Polydispersity index measured by DLS (PDI)	0.10 ± 0.04	0.20 ± 0.04
Ag concentration FAAS (Concentration mg L^{-1})	11.5 ± 1	20.0 ± 2

*Key to annotations: TEM: transmission electron microscopy, AFM, atomic force microscope, DLS: dynamic light scattering, FAAS: flame atomic absorption spectrometer

2.3 Microcosm Experiments

The fate and behavior of AgNPs was assessed in aquatic microcosms. The microcosms are cylindrical columns made of polystyrene plastic and measuring 100 cm in height, 25 cm in diameter and 43 L in volume. The columns were shielded from light in all experiments, by wrapping the exterior walls in foil. AgNPs were introduced as a single concentration pulse through a mesh at a depth of 5 cm below the surface water (Figure SI.12). The starting mass of AgNPs (M_{Ag}) added to the columns (4.3 mg) was estimated to give a final concentration of 100 µg L^{-1} Ag, assuming uniform distribution of Ag throughout the water column and no losses. This Ag mass was introduced as 390 ml of 11 mg L^{-1} cit-Ag NPs, or 215 ml of 20 mg L^{-1} PVP-Ag NPs. The concentration of AgNPs was selected to be as close as possible to predicted environmental concentrations of AgNPs[5], while maintaining sufficient particle concentration to enable analysis. To determine the minimum detectable concentration of AgNPs by UV-vis spectra were collected on AgNPs following serial dilutions, which suggested that a minimum concentration of 50 µg L^{-1} was required for detection (Figure SI.10). The fate and transport of AgNPs was investigated in three media: 1) UPW, 2) EPA moderately hard water (MHW), and 3) EPA moderately hard water spiked with 1 mg L^{-1} Suwannee River fulvic acid (MHW-

SRFA). For lakes and surface waters the expected total organic carbon ranges between 1-30 mg L^{-1}, depending on the trophic state (Hendricks 2006, Thurman 2012). As lower concentrations are more frequent, it was decided that the concentration would be at the lower end of the scale at 1 mg L^{-1}.

All microcosm experiments were performed in triplicate. The MHW was prepared according to guidelines from the United States Environmental Protection Agency (US EPA, 2002) (Table SI.2). The MHW-SRFA was prepared by adding SRFA stock to the MHW and leaving for 24 hours.

Water samples of 5 mL were collected at the introduction point (water surface), middle (50 cm from the surface and bottom), and bottom (90 cm from the surface) of the microcosm column. Water samples were collected using six inch stainless steel hypodermic needles which were permanently fixed to the sampling points. The sampling point at the bottom was always sampled at a 45^{o} angle downwards in order to obtain samples that were within 1 cm of the bottom of the microcosm. No mixing was performed and mesocosms were kept at room temperature (21 ± 2^{o}C). Water samples were collected at different time points following introduction of Ag NPs; 0, 0.5, 1.5, 3.5, 5.5, and 8 hours on day 1 and then on daily-basis for the first 14 days, then again on days 21 and 28. Additionally, samples from the surface and bottom were analysed on days 1-14, 21 and 28, to assess the dissolved and particulate concentration (% Ag) using ultrafiltration methods using a Millipore stirred ultrafiltration cell with a cellulose membrane of 1 kDa (purchased from Sigma) under nitrogen (N_2) gas at approx 14 PSI. Ultrafiltration membrane viability tests were performed by running a set of known standards and checking their recovery rates, by measuring the Ag concentration in the retained and filtrate content. Thus, any adsorbed Ag to the membrane was accounted for in the recovery calculations. All water samples were analyzed for total Ag concentrations by atomic absorption spectroscopy (AAS), and for AgNP aggregation by UV-vis(Baalousha, Nur et al. 2013) and confirmed by TEM analysis.

2.4 Modeling the transport of Ag

As the water in the column was kept stagnant throughout, the transport of AgNPs in the microcosms is determined by their sedimentation after aggregation and their

diffusion. These transport processes can be modeled by the diffusion-sedimentation equation(Socolofsky and Jirka 2005) (Eq 1).

$$\frac{\partial C}{\partial t} + \frac{\partial \mu_i C}{\partial x_i} = D\frac{\partial^2 C}{\partial x_i^2} \quad \text{[Eq 1]}$$

Where D is the diffusion coefficient (m^2 s^{-1}) of the AgNPs or their aggregates, C is concentration (mg L^{-1}), t is time following AgNP introduction, viscosity of the solution μ (Pa.s), and x is the distance AgNPs travelled into the column from the introductory point. To calculate Ag concentration profile as a function of time at the sampling point in the water column, we used a simple analytical solution for Eq 1 that satisfies the experimental boundary conditions. These boundary conditions are: 1) absence of AgNPs in the water column at t = 0; that is C_{Ag} = 0 at t = 0 for 0 < x <L, 2) introduction of AgNPs at the top of the water column; that is C_{Ag} = C_0 at t = 0 and x =0, and 3) no flux at the bottom of the column; that is dC/dx= 0, at x=L. Using these boundary conditions, the analytical solution of Eq 1 can be given by Eq 2:

$$C(x,t) = \frac{M}{A\sqrt{4\pi Dt}}\left(\exp\left(-\frac{(x-x_0)^2}{4Dt}\right) + \exp\left(\frac{(x-x_i)^2}{4Dt}\right)\right) \quad \text{[Eq 2]}$$

Where x_0 is the point where the NPs are introduced to the column, A is column cross section area, and M is the mass of the introduced AgNPs. The nanoparticle diffusion coefficient and sedimentation velocity can be described by Stokes-Einstein (Eq 3) and Stokes equation(Hinderliter, Minard et al. 2010) (Eq 4):

$$D = \frac{KT}{3\pi\mu d} \quad \text{[Eq 3]}$$

$$U = \frac{g(\rho_\rho - \rho_f)d^2}{18\mu} \quad \text{[Eq 4]}$$

Where k is Boltzman constant (m^2 kg s^{-2} K^{-1}), T is temperature (K), μ is medium viscosity (kg m^{-1} s^{-1}) and d is particle diameter (m). The sedimentation velocity is U (m s^{-1}), g is the gravitational force (m s^{-2}), particle density is ρ_ρ (kg m^{-3}) and fluid density is ρ_f, (Hinderliter, Minard et al. 2010). These constant values are described in Table 2.

Table 2: Constant values used in the model

Unit	Constant value	Description
g	9.81	Acceleration of gravity (m s^{-2})
Pp	10490	Density of the particle (kg m^{-3})
Pf	998	Density of the medium (kg m^{-3})
K	1.38065 $X10^{-23}$	Boltzman constant (m^2 kg s^{-2} K^{-1})
T	293.15	Temperature ^oK
μ	0.001	Viscosity of medium(Pa.s) = kg ($m^{-1}s^{-1}$)

This analytical solution can only be used to predict the concentration of AgNPs in the water phase and does not account for particle accumulation at the bottom of the mesocosm following sedimentation/settling on the microcosm floor. Additionally, this analytical solution accounts only for NP diffusion and sedimentation and does not take into account AgNP dissolution and losses of Ag due to sorption on to the solid wall surfaces. Therefore, discrepancies between data and model can be explained partially by dissolution and sorption. The measured concentrations were then fitted using Eq 2, which is essentially an analytical solution of the diffusion-sedimentation model (Eq 1). The fitting parameters that changed were the particle size and concentration, and the rest of the values remained constant.

The weighted sum of squared errors was calculated using Eq 5:

$$X^2 = \sum \frac{(O-E)^2}{\sigma^2} \qquad \text{[Eq 5]}$$

Where σ^2 is the variance of the measured Ag concentrations, O is the observed concentration data, and E is the expected Ag concentration data. The fitting parameters (nanoparticle diameter and mass of Ag introduced to the water column) were optimized by Solver software in Microsoft Excel by minimizing the weighted square error. The middle point data were used in the fitting process as these concentrations are likely to be most accurate concentrations. The top sampling point can be affected by mixing with the water in the introduction reservoir, whereas the bottom sampling point concentrations could be impacted by particle sedimentation.

3 Results and Discussion

3.1 Behavior and Transport of PVP-AgNPs

In all media, PVP-AgNP behaviour followed a pattern broadly consistent with diffusion dominated transport(Tejamaya, Römer et al. 2012). The Ag concentration profiles in UPW, MHW and MHW-SRFA for each of the three sampling points are presented in Figure 1. As described above (section 2.3), all microcosms were spiked with a total mass of Ag NPs that should result in a final concentration of 100 µg L^{-1} Ag in the water column, assuming uniform distribution of Ag throughout the water column and no losses. The total Ag concentration profiles in figures 1A, 1D and 1G, in each water condition, show that the average maximum concentration at the surface sampling point reaches 50 ± 5 µg L^{-1} after 120 hours, where it remains constant for the duration of the study. Time 0 represents the first 5 minutes after sample introduction due to the time taken to sample each depth and microcosm column. This time lapse accounts for the low concentrations of Ag detected at time 0 in both the middle (Figures 1b,1E and 1H) and bottom sampling points (Figures 1C, 1F, and 1I). Due to the immediate mixing of the AgNPs on introduction, it is possible for the rapid diffusion of ionic species, which would account for the measured small Ag concentrations in the lower depths at time 0. On the other hand, particle dispersion is a much slower process (as shown by the higher concentrations of Ag held in the surface water up to 96 hours, and as a result, after ca. 50 hours, both the middle and bottom sampling points show the total Ag concentration increased to reach a plateau of 50 ± 15 µg L^{-1}. It may thus be concluded that the behavior is the same throughout the microcosm columns and conditions, showing losses of approximately 50-70 % from the expected 100 µg L^{-1} Ag concentration. In addition to the analytical limitations, losses of Ag may have occurred from the sorptive losses of the AgNPs to the walls. The total Ag concentration profiles were also fitted with Eq 2 to produce a predicted concentration over time based on particle size and the mass of Ag introduced to the water column (M_{Ag}) (Figures 1 and Table 3). The parameters were based on particle sizes between 11 and 20 nm.The M_{Ag} was between 1.4 and 2.4 mg to reflect the range of concentrations resulting from losses as previously discussed during sampling (especially from areas of high concentration) and

sorption. Ultrafiltration was used as a qualitative measure of the proportion of AgNP transformations in the surface and bottom depths. Ionic Ag (Ag^+) and AgNP data is presented in the supporting information (Tables SI.3, SI.5 and SI.7). In all conditions, over the 28 day study period, PVP-AgNPs accounted for at least 75% of the total Ag concentration in the surface water and 70% in the bottom depth.

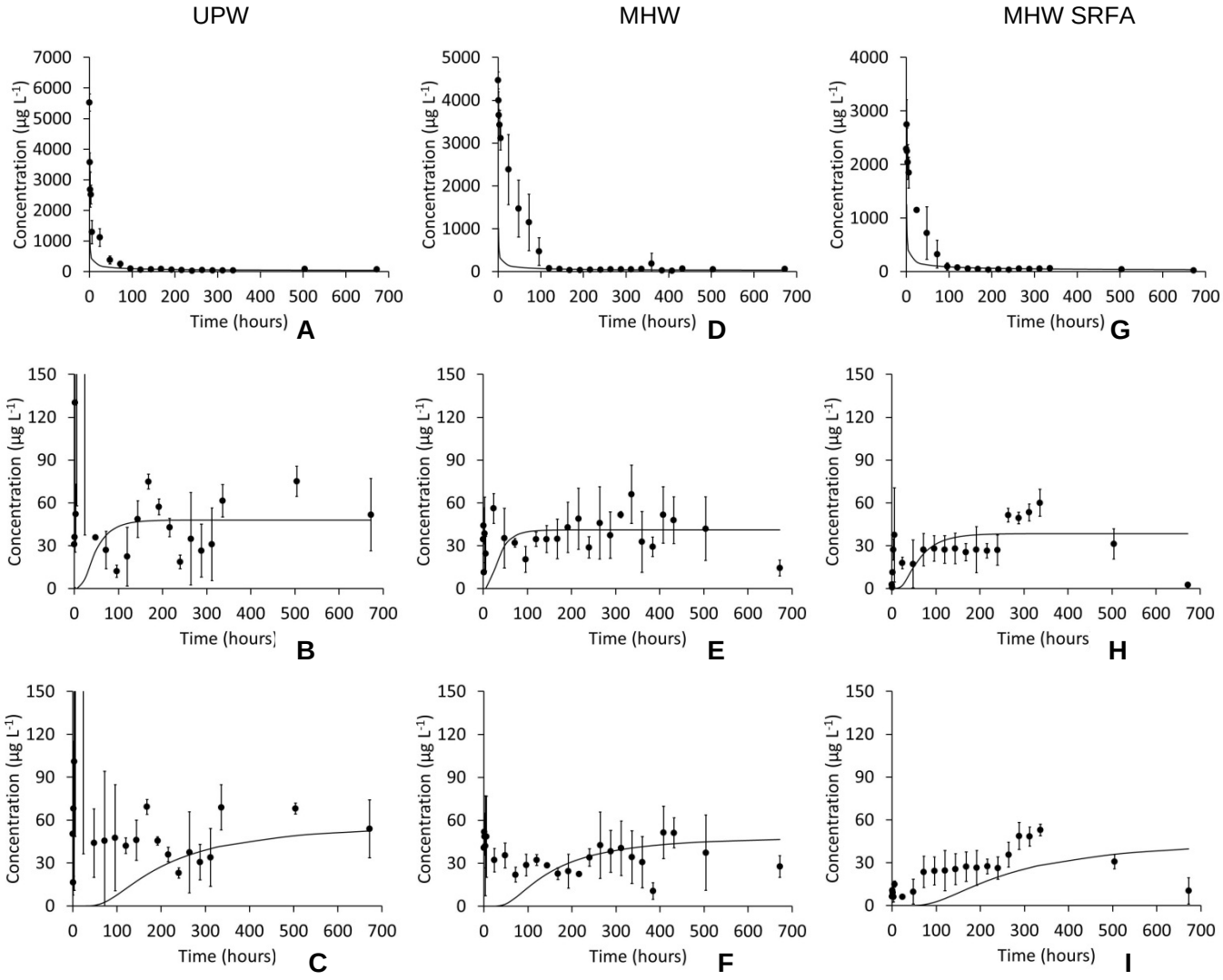
UPW
MHW
MHW SRFA
Surface
Middle
Bottom
Concentration (µg L-1)
Time (hours)
A
B
C
D
E
F
G
H
I

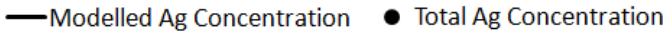

Figure 1: Observed and modelled total Ag concentrations over time for the PVP AgNP study in the surface, middle and bottom depths of the mesocosm, in each of the water conditions (parameters in supporting information) A) UPW surface water, B) UPW middle depth water, C) UPW bottom depth water, D) MHW surface water, E) MHW middle depth water, F) MHW bottom depth water, G) MHW SRFA surface water, H) MHW SRFA middle depth water and I) MHW SRFA bottom depth water. Dots show the average concentrations of three independent triplicates, error bars represent the standard deviation of the measured concentrations in the three replicated and the solid lines is the fitted model. Mass of Ag NPs introduced to the column fixed at 4.3 mg.

Collectively, all the UV-vis spectra for the PVP-AgNPs (Figure 2) show one uniform peak centered on 400 nm, comparable to the 'as prepared PVP-AgNPs (Figure SI.1) and is indicative of unaltered AgNPs[(Tejamaya, Römer et al. 2012),(Römer, White et al. 2011)]. The differences in the UV-vis absorbance maximum (λ_{max}) was also used to trace AgNP movement throughout the microcosms, showing as the λ_{max} absorbance decreased over time from the surface sampling point, the λ_{max} increased in the middle and bottom areas, indicating the migration of PVP-AgNPs into the column. The migration of PVP-AgNPs corresponds with the time trends shown in the modeled and observed Ag concentration data (Figure 1), as the AgNPs move through the microcosm. Losses and reduction in SPR spectra can also be used to indicate dissolution of AgNPs when total Ag concentrations remain unchanged. In all cases the SPR was still detectable at each sampling point at the end of the 28 day study showing particle presence.

To provide further understanding of the PVP-AgNP fate behavior, TEM analysis was conducted on samples of PVP-AgNPs collected from the surface and bottom sampling areas at selected time intervals (Figure 3). All reported TEM sizes were consistent with our experimental data and in agreement with the average particle sizes within the error of measurements and high diffusion coefficients compared to settling velocities (Table 3) used to fit the model data for each water condition.

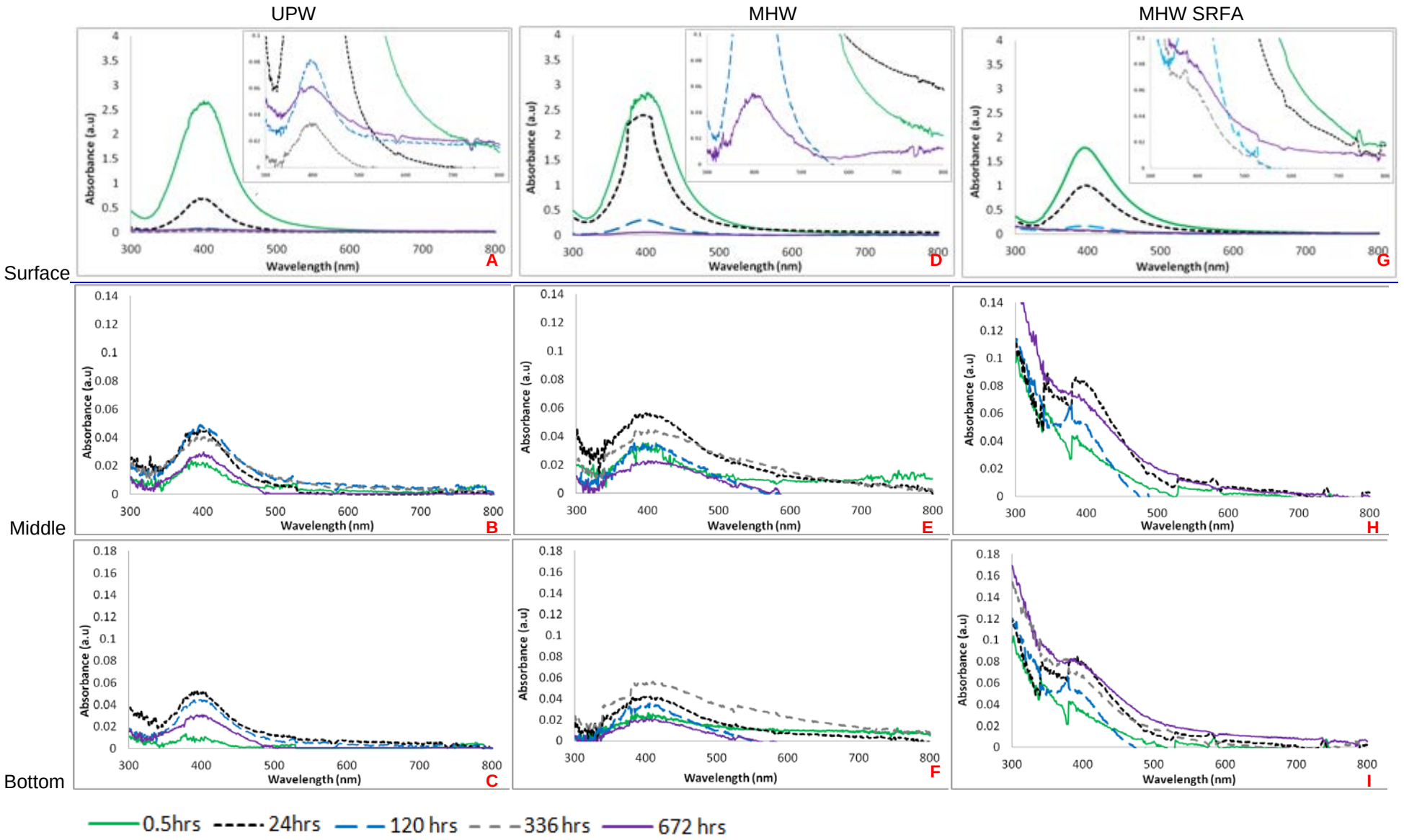

Figure 2: comparison SPR profiles of PVP AgNP over time for the surface, middle and bottom depths of the mesocosm, in each of the water conditions, A) UPW surface water, B) UPW middle depth water, C) UPW bottom depth water, D) MHW surface water, E) MHW middle depth water, F) MHW bottom depth water, G) MHW SRFA surface water, H) MHW SRFA middle depth water and I) MHW SRFA bottom depth water.

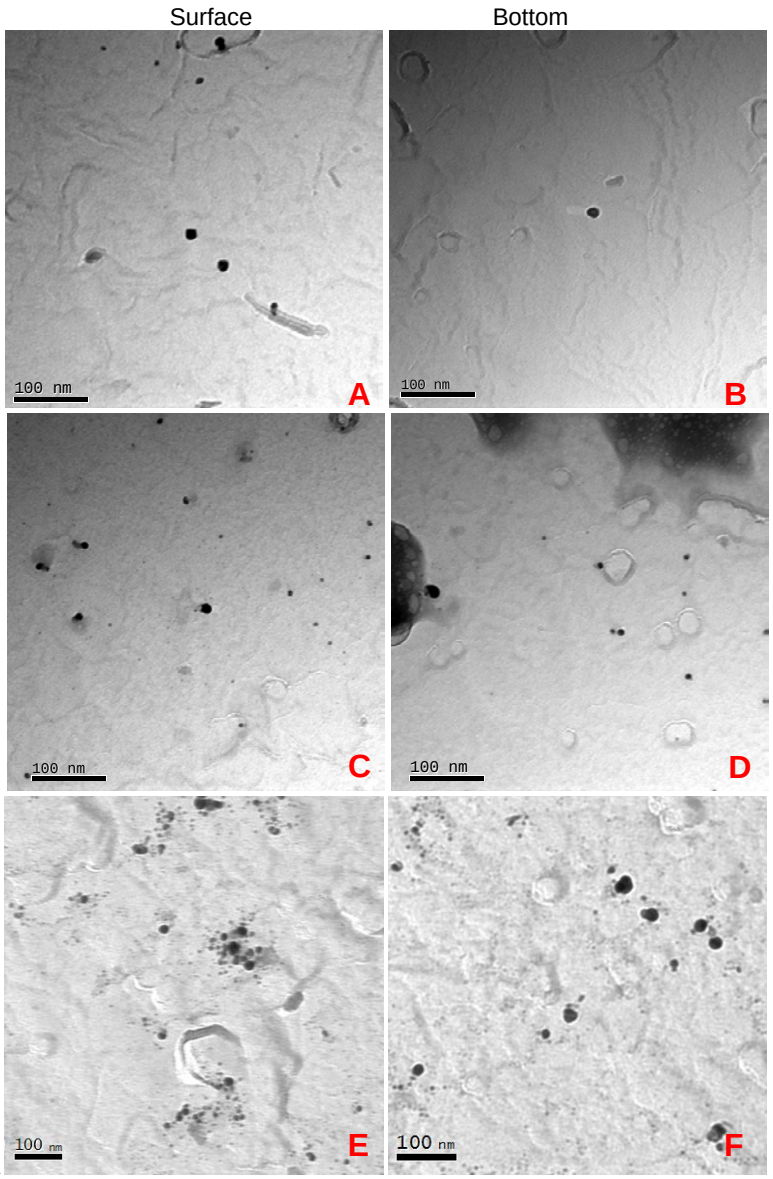

Figure 3: TEM imaging of PVP AgNPs recovered after 24 hours in each of the water conditions, A) surface UPW, B) bottom UPW, C) surface MHW, D) bottom MHW, E) surface MHW SRFA and F) bottom MHW SRFA.

Table 3. Silver mass, diameter, diffusion coefficient and settling velocity calculated by fitting the measured concentration using the diffusion-sedimentation equation

	M_{Ag} (mg)	d (nm)	D (10^{-12} m^2s^{-1})	U_s (10^{-8} m s^{-1})
PVP-Ag NPs				
UPW	2.4	20	21.5	0.21
MHW	2.0	14.8	28.9	0.11
MHW-SRFA	1.4	11	39	0.06
Cit-Ag NPs				
UPW	4.0	10.0	43	0.05
MHW	2.0	88.4	4.9	4.0
MHW-SRFA	3.2	12.7	33.7	0.08

M_{Ag} mass of Ag introduced to the water column (mg), D diffusion coefficient, *v* settling velocity, d diameter (nm)

3.1.1 Behavior of PVP-AgNPs in UPW

To assess the stability and migration behavior of the PVP-AgNPs in UPW the model parameters were optimized using the weighted sum of squared errors (Eq 5) to produce a best fit using a 20 nm particle size and M_{Ag} of 2.4 mg L^{-1} (Table 3). The decrease in M_{Ag} from the starting M_{Ag} (4.3 mg L^{-1}) reflects the potential losses of Ag during sampling and from sorption on to the solid surfaces of the microcosm. The diffusion coefficient of the modeled particles was 21.5 X 10^{-12} m^2s^{-1} exceeding the sedimentation velocity of 0.21 X 10^{-8} m s^{-1} (Table 2), evidencing that diffusion was the dominant migration process. The higher diffusion coefficient confirms diffusion dominated migration and thus, the maintained stability of the PVP AgNPs when released into the UPW. Furthermore, the small NP size (20 nm) used to produce the best fit for the modeled Ag concentration is reflective of the PVP AgNP stability and is comparable to the 'as prepared' PVP-AgNPs. In addition to the model parameters, the observed total Ag concentration profiles (also presented in Figures 1A, 1B and 1C) for the UPW conditions, show the Ag concentrations between each sampled depth were comparable at each time point and satisfy the rules of Stokes-Einstein Law of particles in solution(Hinderliter, Minard et al. 2010) and Ficks Law of diffusion(Fick 1855, Gorban, Sargsyan et al. 2011). Therefore, this provides suitable evidence to support AgNP dissolution. At any given time, the total Ag concentration accounted for >80% AgNPs and <20% dissolved Ag throughout the study in UPW (Table SI.3).

UV-vis is a particularly important tool used to identify changes in AgNP properties, which can alter their SPR. A single UV-vis peak at 400 nm was comparable to the 'as prepared PVP-AgNPs (Figure SI.1) showing characteristics of unaltered AgNPs[(Tejamaya, Römer et al. 2012),(Römer, White et al. 2011)]. Additionally the SPR signal was present for 672 hours (28 days) confirming their presence and

stability. TEM imaging (Figures 3A and 3B) also identified small single spherical particles in the surface and bottom depth of the microcosm at 24 hours post release. The average size was 13 ± 7 nm in the surface and 14 ± 4 nm in the bottom, showing no significant difference (Table SI.4) when compared to the as prepared PVP-AgNPs prior to release and agrees with the model size fitting parameters. The TEM imaging produced both qualitative and quantitative information which underpins the model concentrations and the UV-vis data to provide strong evidence that PVP-AgNPs remain stable in UPW. These results are also in agreement with previous findings for small sterically-stabilized AgNPs in UPW(Liu and Hurt 2010), therefore diffusion dominated transport was used to show accurate calibrations for the model.

3.1.2 Behavior of PVP-AgNPs in MHW

When the PVP-AgNPs were released into the MHW (Figures 1D, 1E and 1F), the modeled fitting parameters (*ca.* d and M_{Ag}) were appropriate to confirm unaltered particles. The weighted sum of squared errors (Eq 5) optimized the model fits, using a small average size of 14.8 nm (consistent with TEM size analysis) and a M_{Ag} of 2 mg L^{-1}. The optimized model sizes were also comparable to the 'as prepared AgNPs'. The diffusion coefficient of 28.9 X 10^{-12} m^2s^{-1} was higher when compared to the sedimentation velocity of 0.11 X 10^{-8} m s^{-1} (Table 3). This information supports that PVP AgNPs maintained stability and migrated through the microcosm columns via diffusion, in a similar fashion to the behavior observed in UPW.

It is well documented in the literature that in simple aqueous environments AgNPs form complexes with cholride chloride and sulfide ligands(Lowry, Gregory et al. 2012, Tejamaya, Römer et al. 2012, Peijnenburg, Baalousha et al. 2015),(Levard, Reinsch et al. 2011), which were all present in the MHW, although no evidence for their co-existance was found here, in contrast with cit-AgNPs (see section 3.2.2.). In addition, there was some evidence of Ag dissolution and reprecipitation during the study, as 71% of the total Ag concentration was accounted for NPs after 24 hours (Table SI.5), compared to 81% on day 28. The co-existence of Ag and Cl present the possibility for precipitation of (most probably) AgCl nanoparticles, as a transformation process (as observed in the EDS profiles in Figure 7B). As AgCl NPs do not have an associated SPR absorbance (Zook, Long et al. 2011), it was not possible to qualitativly identify this association, although the co-existance of the AgCl may explain the slight vairations in size.

Despite some dissolution and the influence of the water chemistry, a total Ag concentration remained comparable between each depth (surface, middle and bottom) at 120 hours (5 days (Figures 1D, 1E and 1F) and for the duration of the study thereafter.

SPR is a good indicator of aggregation of AgNPs(Baalousha, Nur et al. 2013) where additional second absorbance peaks in the region of 500-700 nm confirm the presence of larger particulates(Chinnapongse, MacCuspie et al. 2011, Baalousha, Nur et al. 2013). UV-vis spectra for the PVP-Ag NPs (Figure 2D, 2E, and 2F) show only a single peak in each depth at 400 nm which remains constant for the duration of the study over 672 hours (28 days), which confirms the stability of the PVP-AgNPs. Morphological observations (Figure 3C and 3D) confirm the presence of small spherical particles and measuring 13 ± 8 nm in the surface and 16 ± 6 nm in the bottom post 24 hours release (Table SI.6). These figures are also in agreement to the sized used to fit the model parameters.

3.1.3 Behavior of PVP-AgNPs in MHW-SRFA

Evidence for the presence of unaltered PVP-AgNPs in the MHW-SRFA was provided by the optimized model parameters which used particle size of 11 nm and a M_{Ag} of 1.4 mg to create a best fit (Eq 5) between our observed and expected total Ag concentration profiles (Figure 1G, 1H and 1I). The small particle size was comparable to the 'as prepared' PVP-AgNPs and the TEM sizing at 24 hours post release. The model calculated the diffusion coefficient to be 39 $X10^{-12}$ m^2s^{-1} with a sedimentation velocity of 0.06 X 10^{-8} m s^{-1} (Table 3). In agreement to the previous water exposures (in UPW) for the PVP-AgNPs, a higher diffusion coefficient strongly suggests that diffusion was the dominant process of migration. Furthermore, evidence to support particle stability and diffusion dominated transport was shown by a maintained concentration gradient between each depth of the mesocosm after 72 hours (days 3), where concentrations of Ag remained comparable at 35 ± 12 µg L^{-1} for the duration of the study. Figure 2G, H and I show the UV-vis absorbance peaks at 400 nm, although the SPR at 300 nm in 2H and 2I is due to interferences of band tailing at 254 nm from the SRFA (USA,EPA, 2009, (Hendricks 2006). UV absorbance spectra show only the absorbance for SRFA is presented in Figure SI.11 (Supporting information).

Morphological observations of the PVP-AgNPs at 24 hours post release identified small singular particles (Figure 3E and 3F) sized at 11 ± 3 nm (Table SI.8) at the bottom sampling point. Due to insufficient AgNP numbers for statistical relevance, it was not possible to determine size from the surface sampling point. Nonetheless the reported sizes were comparable to those used to produce a best fit from the model for our data, further confirming PVP-AgNP stability in MHW-SRFA.

To conclude, it is likely that the overall stabilty of the PVP-AgNPs is due to the thermodynamics of the high molecular weight structural complexity of PVP polymer forming a thick layer that is strongly bound to the surface of the Ag atom(Kvitek, Panáček et al. 2008). Therefore,

compared to the citrate surface stabilizer, PVP is not sensitive to charge screening under the influence of the simple electrolyte media, maintaining unaltered AgNPs [Tejamaya, Römer et al. 2012),(Badawy, Luxton et al. 2010)], even at high ionic strengths[Kvitek, Panáček et al. 2008),(Ju-Nam and Lead 2008)]. In addition the stability of the PVP AgNPs in the MHW-SRFA may also have been due to NOM adsorption to the particle surface(Auffan, Bottero et al. 2010, Tejamaya, Römer et al. 2012, Hitchman, Smith et al. 2013).

3.2 Behavior and transport of cit-AgNPs

The observed and modeled Ag concentration profiles for the cit-AgNP releases are presented in Figure 4 for each water condition. The UV-vis profiles are presented in Figure 5 and accompanying TEM imaging for each water condition is shown in Figure 6. In contrast to the PVP-AgNPs (Figure 1), the cit-AgNPs behavior and transport was media-dependant.

544

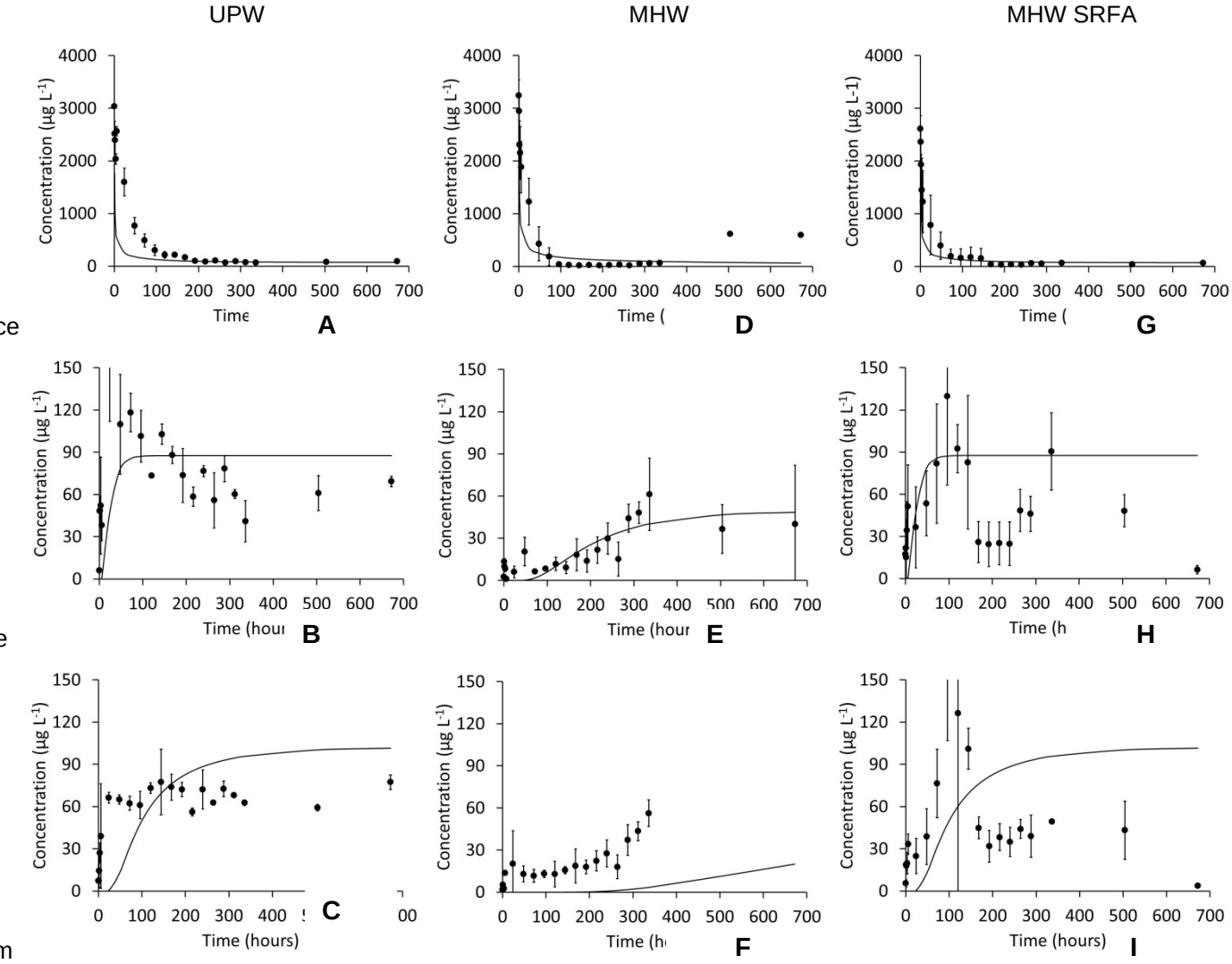

Figure 4: Observed and modelled total Ag concentrations over time for the citrate AgNP study in the surface, middle and bottom depths of the mesocosm, in each of the water conditions (parameters in supporting information). A) UPW surface water, B) UPW middle depth water, C) UPW bottom depth water, D) MHW surface water, E) MHW middle depth water, F) MHW bottom depth water, G) MHW SRFA surface water, H) MHW SRFA middle depth water and I) MHW SRFA bottom depth water. Dots show the average concentrations of three independent triplicates,

error bars represent the standard deviation of the measured concentrations in the three replicated and the solid lines is the fitted model. Mass of Ag NPs introduced to the column fixed at 4.3 mg.

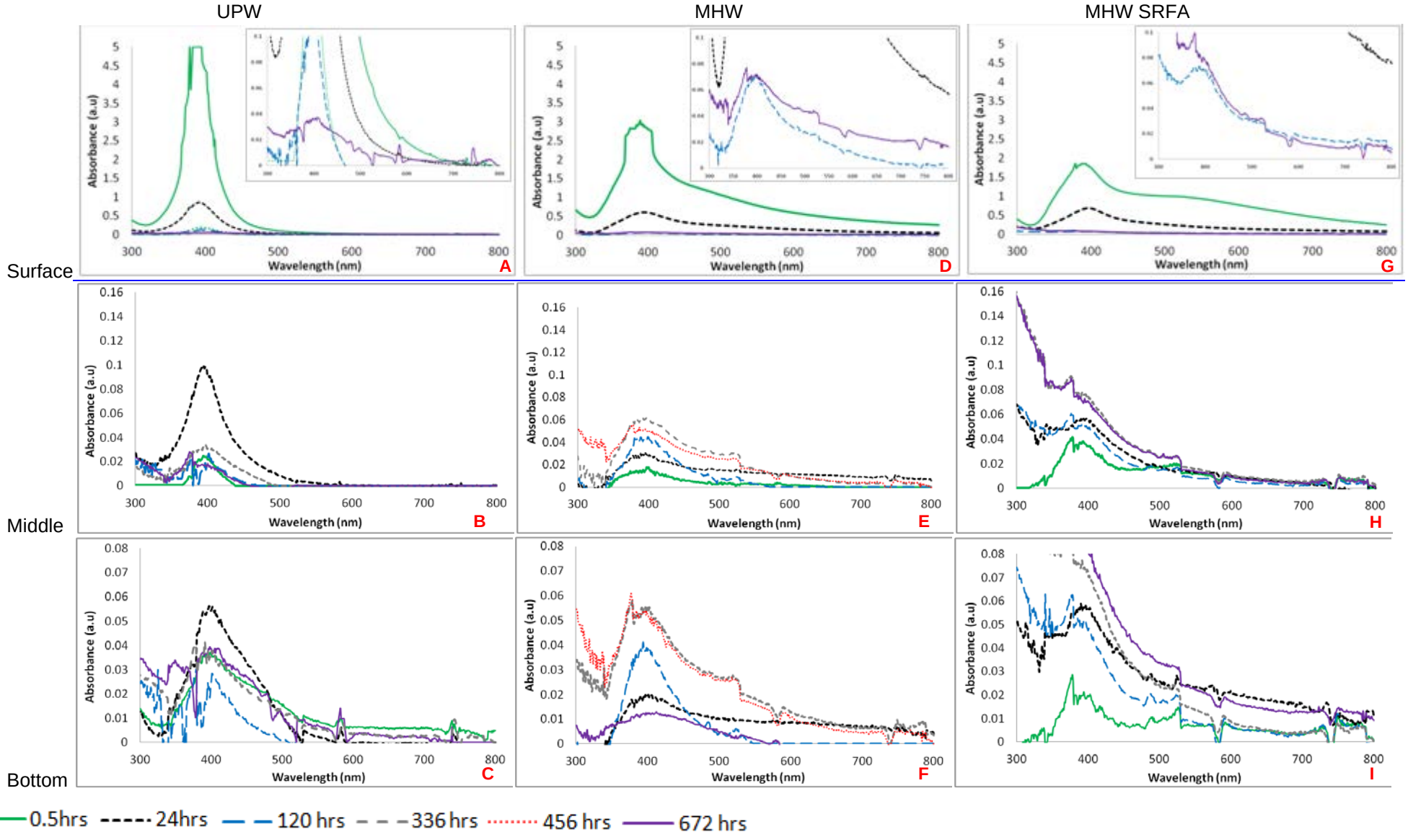

Figure 5: comparison SPR profiles of citrate AgNP over time for the surface, middle and bottom depths of the mesocosm, in each of the water conditions. A) UPW surface water, B) UPW middle depth water, C) UPW bottom depth water, D) MHW surface water, E) MHW middle depth water, F) MHW bottom depth water, G) MHW SRFA surface water, H) MHW SRFA middle depth water and I) MHW SRFA bottom depth water.

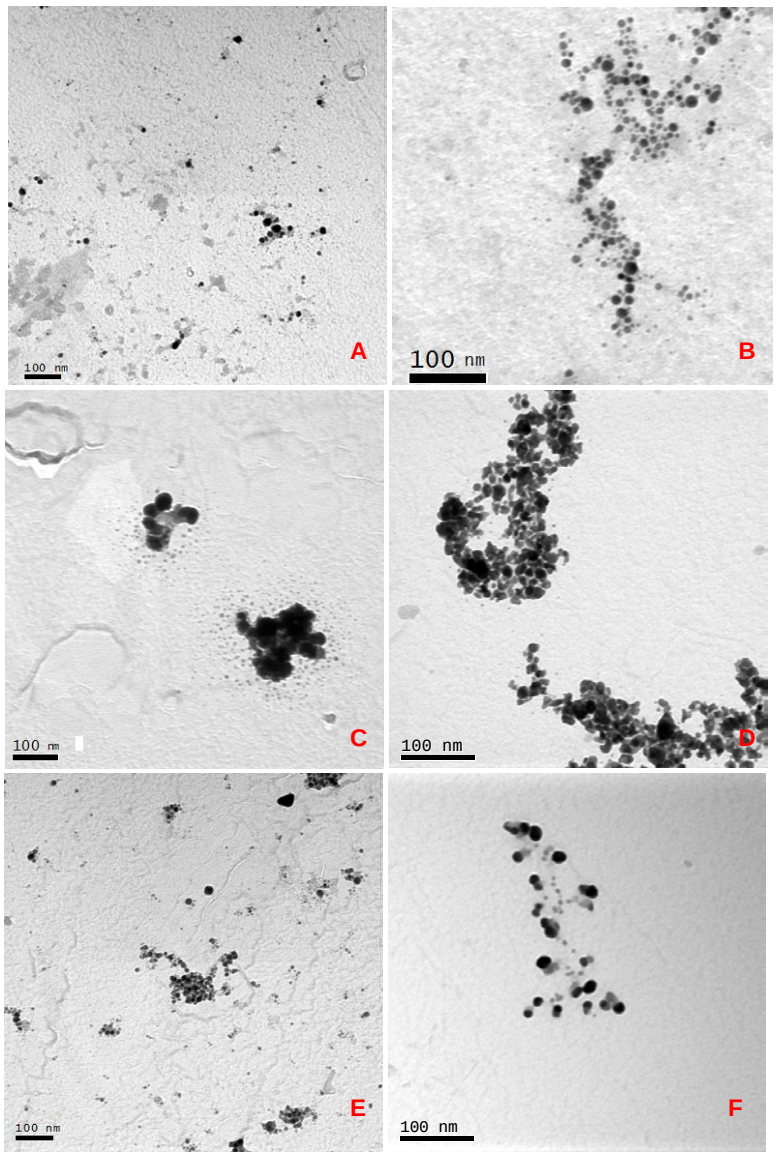

Figure 6: TEM imaging of citrate AgNPs recovered after 24 hours in each of the water conditions, A) surface UPW, B) bottom UPW, C) surface MHW, D) bottom MHW, E) surface MHW SRFA and F) bottom MHW SRFA.

3.2.1 Behavior of cit-AgNPs in UPW

In UPW, the cit-AgNPs remained stable with comparable behavior and transport mechanisms to the PVP-AgNPs, suggesting few transformations in agreement with other studies(Römer, White et al. 2011). To determine stability of the cit-AgNPs the Ag concentration profiles (Figures 4A-C) were fitted (Eq 2), using the weighted square of fitting errors (Eq 5) and the primary particle size of 10 nm with a M_{Ag} of 4 mg. The particle size used was comparable within the error of the measurements to the 'as prepared' cit-AgNPs and in agreement to the TEM sizing (Table SI.4).

The model accurately predicted the total Ag concentrations to identify strong correlations between our observed and expected data using the Chi squared analysis (Eq 5), which were comparable to the PVP-AgNP studies. Table 3 shows a high diffusion coefficient of the 10 nm particles (43 X 10^{-12} m^2s^{-1}) combined with a low settling velocity (0.05 X 10^{-8} m s^{-1}), indicating diffusion orientated behaviour of small NPs in suspension. Dissolution of the AgNPs (Table SI.3) was observed after day 1 in each of the surface and bottom of the microcosms, by measuring dissolved and particulate Ag (ultrafiltration). In the surface, the total Ag concentration accounted for 85% AgNPs and 15% dissolved Ag, whereas, the Ag concentration on day 28 accounted for 63% AgNPs and 37% dissolved Ag.

The UV-vis spectra of cit-AgNPs in UPW shows a single absorption peak centered at 392 nm (Figures 5A, 5B and 5C) for each of the surface, middle and bottom depth. These results confirm the stability of the cit-AgNPs in UPW and are consistent with the literature for small spherical particles[(Cumberland and Lead 2009),(Tejamaya, Römer et al. 2012),(Römer, White et al. 2011)]. The UV-vis spectra of cit-AgNPs also indentified UV-vis SPR peaks at 672 hours (day 28), confirming AgNP presence in each of the surface, middle and bottom sampling points. Additionally, as discussed in section 2.4, the model inputs do not take into account AgNP dissolution and losses of Ag. Therefore discrepancies between the model and observed total Ag concentration data with the UV evidence can be explained partially by dissolution and sorption. However, since the modeled particle size remains comparable to the 'as prepared' cit-AgNPs (within the error of measurement) the model size values and diffusion coefficient are valid to confirm the cit-AgNPs remain mostly unaltered in UPW. Furthermore, TEM imaging (Figures 6A and 6B) confirmed single spherical particles in the surface and bottom depth of the mesocosm at 24 hours post release, providing evidence to support the model parameters and that the cit-AgNPs migrated via diffusion dominated transport.

3.2.2 Behavior and transport of cit-AgNPs in MHW

When introduced to the MHW, the yellow/orange color of the cit-AgNPs immediately changed to dark brown/orange. This became colorless as particles migrated and diluted through the columns over the first 0.5 hours. In the presence of simple electrolytes, the visual color changes on release are consistent with the aggregation of cit-AgNPs[(Tejamaya, Römer et al. 2012), (Zhang, Smith et al. 2012)].

The modeled concentration profiles for the cit-AgNPs released in MHW, did not fit with the observed Ag concentrations when modeled with the primary particle size as described for the previous UPW study. A larger size of 88.4 nm produced the best fit for the model (Eq 5), further suggesting media-dependent aggregation (and precipitation) and sedimentation behavior, which account for the concentration rises and declines observed in Figures 4D-F (Socolofsky and Jirka 2005, Hinderliter, Minard et al. 2010). The settling velocity of the cit-AgNPs also increased to 4 $X10^{-8}$ ms^{-1}, whereas the diffusion rate decreased to 4.9 $X10^{-12}$ m^2s^{-1} (Table 3) evidencing sedimentation dominated migration.

Additionally, the total Ag concentration changes over time in the middle and bottom of the microcosm (Figure 4H and 4I), show a systematic trend where the Ag concentration gradually rises to reach a concentration max of 83 ± 15 µg L^{-1} at 336 hours (day 14) before falling to 40 ± 17 µg L^{-1} at 504 hours (day 21) and 30 ± 15 µg L^{-1} at 672 hours (day 28) as the Ag begins to settle. The Ag concentration behavior is indicative of both dissolution and precipitation behavior (Table SI.5), combined with sedimentation dominated AgNP transport (i.e. moving as a cloud of aggregated AgNPs through the column). This concentration profile was not observed in the UPW and MHW PVP-AgNP study, indicating surface coating dependent behavior, as well as media dependent behavior.

After 14 days, the AgNP concentration accounted for only 54% for the total Ag in the surface water. Similarly, AgNPs only contributed to 57% of the total Ag in the bottom at day 14, with the number being slightly higher due to sedimentation. Reprecipitation of AgNPs was evident in the surface water over time, as the AgNP concentration increased from 65% on day 21 to 71% on day 28 (Table SI.5), with no effects to the total Ag concentration. Differences in the cit-AgNP concentration in the surface sampling point over the 28 day study were also accompanied by a reduced SPR peak (Figure 5D), which is consistent with rapid aggregation of cit-Ag NPs(Baalousha, Nur et al. 2013). A UV-vis peak at 392 nm with an additional second absorbance peak in the region of 500-700 nm, also confirmed cit-AgNP instability and aggregation at the surface of the microcosm(Chinnapongse, MacCuspie et al. 2011, Baalousha, Nur et al. 2013). These additional peaks were absent when cit-Ag NPs were released in UPW and for all PVP-AgNP experiments. Furthermore, SPR peaks were only visible in MHW for 456 hours (19 days) in the middle depth compared to 672 hours (28 days) in the UPW exposures, showing a decline in AgNP concentration as they sediment and dissolve.

TEM imaging revealed that the cit-AgNPs in the surface MHW were 13 ± 5 nm after 24 hours (Figure 6C, Table SI.4) and the cit-AgNPs located at the bottom were significantly larger at 23 ± 23 nm (Table SI.6), further evidencing aggregation determined behavior when introduced to an electrolyte containing media. Note that the 88 nm used to model the particle reflects the average core size during the whole time course of the study and does not reflect the changing dissolution and reprecipitation of the NPs. Morphological observations show that the particles were aggregated and larger than those compared to the UPW study at 24 hours in the bottom of the microcosm. EDS (Figure SI.13) confirmed the presence of Ag from the aggregates shown in Figure 6D. The changes that were observed from the TEM imaging between the MHW compared to the UPW are indicative of the physicochemical changes that will incur when exposed to environmental waters.

The EDS spectrum (Figures 7B) identifed the presence of Ca, Mg, S, Cl and Na in solution, all of which could possibly interact with the charged surface of the cit-AgNPs and thus result in aggregation. Particular interest is given to the presence of divalent cations (Ca^{2+} and Mg^{2+}) shown in Figure 7B, as these have been proven to influence cit-AgNP aggregation by bridging between two anionic moleculees. Additionally, aggregation may also have been caused by the cations in solution such as Na and Cl by neutralising surface charge of the citrate stabilizer(Akaighe, Depner et al. 2012). Previous work found that the dilution of AgNPs in media leads to citrate re-equilibration and loss from surface followed by aggregation[20], in agreement with the present study which showed the citrate capping to result in more unstable nanoparticles. Differences between UPW and MHW suggests this mechanism (dilution and loss of citrate) is also important. Studies by Baalousha et al, (2013) and Akaighe et al (2012) further observed aggregation of citrate AgNPs in $CaCl_2$, $MgCl_2$ and $NaCl_2$ containging media ionic strenghts relevant to the present study(Akaighe, Depner et al. 2012).

Coprecipitation with Cl of the AgNPs is also a possible mechanism that would result in increased aggregation(Levard, Hotze et al. 2012). The results from the present study were also similar to EDS profiles obtained by Ha and Payer (2011) who exposed Ag to a sodium chloride solution (NaCl) and obtained AgCl complexes(Ha and Payer 2011). As citrate coated AgNPs are electrostatically stabilized, they are therefore prone to aggregation by charge neutralization caused by the electrolytes present in the MHW water(Bae, Hwang et al. 2013).

As described by the Derjaguin-Landau-Verwey-Overbeek (DLVO) theory, the electrostatic repulsion between two particles in conjunction with van der Waals attraction will determine particle aggregation(Baalousha 2009). Partial removal of the citrate surface coating and a change in the surface charge, induced by ionic strength will reduce the electrostatic diffuse double layer, resulting in increased aggregation(Römer, White et al. 2011). Additionally, UPW does not contain citrate, therefore the re-equilibration of citrate from the NP surface into the aqueous phase, would

also result in the surface coating loss. Furthermore, the lack of charge repulsion between the particle surfaces causes decreased charge shielding, susceptibility to dissolution, and the formation of silver complexes with the electrolytes in solution, such as chloride[(Lowry, Gregory et al. 2012),(Levard, Reinsch et al. 2011),(Levard, Mitra et al. 2013)]. In contrast, the PVP coated AgNPs are sterically stabilized and are more stable in ionic solutions, as the presence of cations do not significantly influence steric stabilization, or induce charge neutralization.

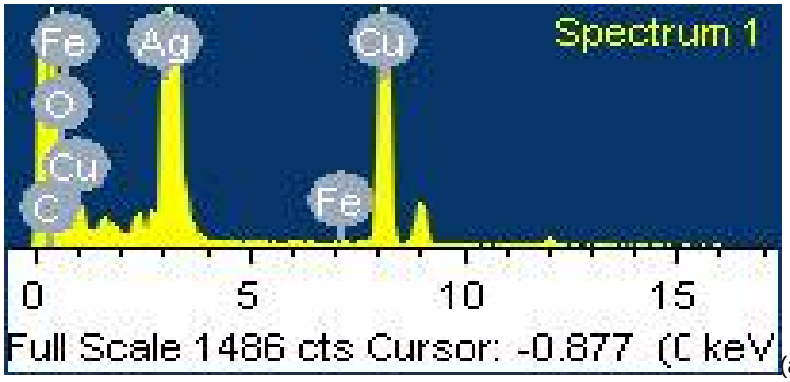

(a)

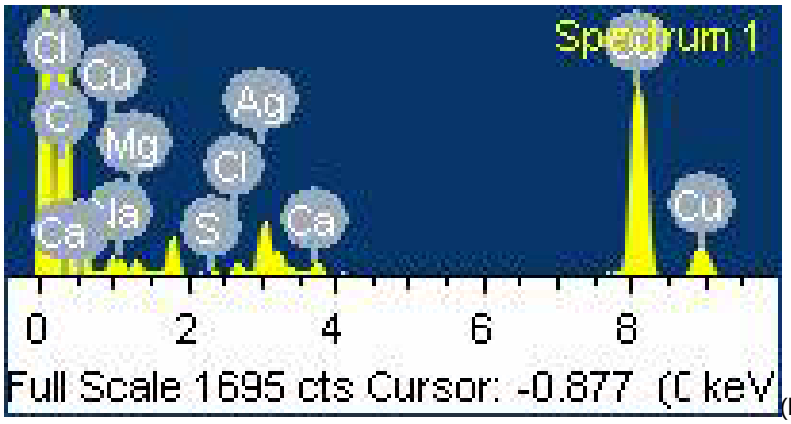

(b)

Figure 7: A) EDX spectra for pristine citrate AgNP suspensions and B) EDX spectrum for cit-AgNPs located in the surface water after 24 hrs exposure to MHW with additional SRFA. The presence of copper (Cu) and carbon (C) shown in the EDS spectrum represent the carbon film and copper mesh grid used to mount the sample.

3.2.3 Behavior of cit-AgNPs in MHW-SRFA

Using Eq 2, we were able to show the stabilizing effects of SRFA by fitting the model parameters (Figure 4G, 4H and 4I) using the weighted square of fitting errors (Eq 5) with a smaller particle size of 12.7 nm, when compared to the MHW study absent of SRFA. The observed stabilizing effects of cit-AgNPs exposed to low concentrations of NOM are also in agreement with previous literature[(Chinnapongse, MacCuspie et al. 2011),(Manciulea, Baker et al. 2009)]. The Ag concentration rises over the first 5 days (120 hours) in the middle depth (Figure 4H) illustrating sedimentation governed behavior as larger particles settle. However, after 168 hours (7 days) the Ag concentration decreased to 30 ± 10 μg L^{-1} which remained consistent until the end of the study. This behavior is conformational of a

mix of sedimentation and diffusion governed transport mechanisms, despite the smaller modeled size. Additionally this behavior also predicts that the mobility of the cit-AgNPs in natural environments will be influenced by adsorption/deposition onto solid objects such as suspended solids (NOM), soil sediments and organisms, thus reducing their bioavailability and migration (Auffan, Bottero et al. 2010, Bae, Hwang et al. 2013).

After 24 hours, the AgNP concentration was higher accounting for 89% of the total Ag in the surface water and 95% in the bottom depth, compared to the previous cit-AgNP studies. The data from Table SI.7 (Supporting Information) suggests the SRFA has reduced the effects of dissolution, although, the higher AgNP concentration in the bottom is indicative of immediate sedimentation, which may have been caused by deposition of the cit-AgNPs on to the SRFA. Aggregation was also confirmed in the UV-vis spectra (Figure 5G,5H and 5I) where a second absorbance peak in the region of 500-700 nm at 0.5 hours was present in the surface water[(Chinnapongse, MacCuspie et al. 2011),(Baalousha, Nur et al. 2013)]. Aggregation of the cit-AgNPs in the presence of SRFA may be caused by bridging flocculation(Huynh and Chen 2011) and is consistent to findings by Quik et al, 2014 who observed the sedimentation of nanoparticles in a range of natural waters(Quik, Velzeboer et al. 2014). However, the additional second absorbance peaks were no longer present in the middle or bottom depths after this time point, confirming sedimentation and sorption(Bae, Hwang et al. 2013). Additionally, the absence of these UV-vis bands at later sampling points are consistent with the smaller modeled size and previous literature[(Cumberland and Lead 2009),(Tejamaya, Römer et al. 2012)].

NOM has been documented to displace the citrate surface stabilizer by re-coating the particle with NOM (Diegoli, Manciulea et al. 2008) to provide steric stabilization(Baalousha, Manciulea et al. 2008), which has been evidenced in the present study. The steric stabilization from the addition of the SRFA to the MHW enhanced the stability and persistence of the citrate AgNPs in the surface waters by reducing aggregation, which was not observed in the MHW absent of SRFA. Reduced aggregation and sedimentation of the cit-AgNPs was complimented by the reduced SPR banding patterns between 600-800 nm in figures 4G, 4H and 4I after 24 hours, compared the MHW absent of SRFA (Figures 5D, 5E and 5F).

Although stabilization of the cit-AgNPs was observed, the formation of aggregates in the presence of SRFA can be explained either by reprecipitation of AgNPs and/or the charge neutralization, charge screening or bridging flocculation(Huynh and Chen 2011) of the SRFA on the AgNP surfaces. SRFA can act as a reducing agent, to nucleate ionic Ag to grown into elemental Ag coated by the NOM (Akaighe, Depner et al. 2012). TEM imaging continued to support the stabilizing effects of the addition of SRFA to the MHW standard (Figure 6E and 6F). The aggregate structure in figures 6E and 6f are morphologically different to those observed in figure 6D, showing small spherical particles closely connected by a surface film similar to those

observed in Baalousha et al (2009)(Baalousha 2009), compared to core 'fusion' of the NP aggregates observed in Figure 6d. Cit-AgNPs had an average TEM size of 12 ± 6 nm (Table SI.8) in the surface water comparable to the primary particle size, and were larger in the bottom area at 27 ± 10 nm 24 hours post release (Table SI.8: Figure 6E). Results show a reduction in size compared to those observed in the MHW absent of SRFA, demonstrating stability in the presence of NOM.

4 Conclusions

In all conditions, sorption of Ag to the microcosm wall was responsible for Ag concentration losses, suggesting that sorption of particulates might be a dominant behavior when AgNPs are released in to the environment. PVP-AgNPs remained unaltered, regardless of the chemical composition of the water matrix and displayed diffusion dominated transport behaviors. The model data used both the primary 'as prepared' sizes and the reported TEM aggregate sizes (cit-AgNPs) to help validate the transport mechanisms in each study. Further evidence of non-aggregated spherical AgNPs was shown from the TEM imaging and SPR data to support the stability and diffusion of the PVP AgNPs over the citrate AgNPs.

Cit-AgNPs were only stable in the UPW studies, whereas ionic concentrations measured in the presence of cit-AgNP indicated complex mass fluctuations, sedimentation dominated migration and potential reprecipitation of AgNP species. These behaviours and transformations are all likely to be dominant when released in real water conditions. The addition of SRFA demonstrated small stabilizing effects to the cit-AgNPs which was validated in the model and TEM imaging where the primary particle sizes compared to the 'as prepared' AgNPs used. The total Ag concentration losses also suggest that eventually the AgNPs will either adsorb to NOM and other surfaces and/or sediment.

Based on the information presented in this study we can make predictions that concentrations of AgNPs will be elevated in waters with higher concentrations of NOM, due to the displacements of electrostatic surface coating and sorption of NOM onto the AgNP surface to enhance their stability. AgNPs will also interact with chlorine and sulphur species in natural waters and this may enhance their persistence in environmental conditions. Waters with lower NOM concentrations and higher electrolyte concentrations will favor aggregation mechanisms of electrostatically coated particles and particles with no surface modifications. Aggregated particles will sediment and are likely to be bioavailable to sediment-dwelling organisms with potential implications to this ecological niche.

Acknowledgments

We would like to thank the Natural Environment Research Council (NE/H013148/1) and the Centre for Environmental Nanoscience and Risk (CENR) for their financial support.

References

Akaighe, N., S. W. Depner, S. Banerjee, V. K. Sharma and M. Sohn (2012). "The effects of monovalent and divalent cations on the stability of silver nanoparticles formed from direct reduction of silver ions by Suwannee River humic acid/natural organic matter." Science of the Total Environment **441**: 277-289.

Auffan, M., J.-Y. Bottero, C. Chaneac and J. Rose (2010). "Inorganic manufactured nanoparticles: how their physicochemical properties influence their biological effects in aqueous environments." Nanomedicine **5**(6): 999-1007.

Baalousha, M. (2009). "Aggregation and disaggregation of iron oxide nanoparticles: Influence of particle concentration, pH and natural organic matter." Sci Total Environ **407**(6): 2093-2101.

Baalousha, M., K. Arkill, I. Romer, R. Palmer and J. Lead (2015). "Transformations of citrate and Tween coated silver nanoparticles reacted with Na 2 S." Science of The Total Environment **502**: 344-353.

Baalousha, M. and J. Lead (2012). "Rationalizing nanomaterial sizes measured by atomic force microscopy, flow field-flow fractionation, and dynamic light scattering: sample preparation, polydispersity, and particle structure." Environmental science & technology **46**(11): 6134-6142.

Baalousha, M. and J. Lead (2013). "Characterization of natural and manufactured nanoparticles by atomic force microscopy: Effect of analysis mode, environment and sample preparation." Colloids and Surfaces A: Physicochemical and Engineering Aspects **419**: 238-247.

Baalousha, M., A. Manciulea, S. Cumberland, K. Kendall and J. R. Lead (2008). "Aggregation and surface properties of iron oxide nanoparticles: influence of pH and natural organic matter." Environmental Toxicology and Chemistry **27**(9): 1875-1882.

Baalousha, M., Y. Nur, I. Römer, M. Tejamaya and J. Lead (2013). "Effect of monovalent and divalent cations, anions and fulvic acid on aggregation of citrate-coated silver nanoparticles." Science of the Total Environment **454**: 119-131.

Badawy, A. M. E., T. P. Luxton, R. G. Silva, K. G. Scheckel, M. T. Suidan and T. M. Tolaymat (2010). "Impact of environmental conditions (pH, ionic strength, and electrolyte type) on the surface charge and aggregation of silver nanoparticles suspensions." Environmental science & technology **44**(4): 1260-1266.

Bae, S., Y. S. Hwang, Y.-J. Lee and S.-K. Lee (2013). "Effects of water chemistry on aggregation and soil adsorption of silver nanoparticles." Environmental health and toxicology **28**.

Balnois, E. and K. J. Wilkinson (2002). "Sample preparation techniques for the observation of environmental biopolymers by atomic force microscopy." Colloids and Surfaces A: Physicochemical and Engineering Aspects **207**(1): 229-242.

Benn, T. M. and P. Westerhoff (2008). "Nanoparticle silver released into water from commercially available sock fabrics." Environmental science & technology **42**(11): 4133-4139.

Chen, K. L. and M. Elimelech (2007). "Influence of humic acid on the aggregation kinetics of fullerene (C 60) nanoparticles in monovalent and divalent electrolyte solutions." Journal of Colloid and Interface Science **309**(1): 126-134.

Chinnapongse, S. L., R. I. MacCuspie and V. A. Hackley (2011). "Persistence of singly dispersed silver nanoparticles in natural freshwaters, synthetic seawater, and simulated estuarine waters." Science of the total environment **409**(12): 2443-2450.

Cumberland, S. A. and J. R. Lead (2009). "Particle size distributions of silver nanoparticles at environmentally relevant conditions." Journal of Chromatography A **1216**(52): 9099-9105.

Dale, A. L., E. A. Casman, G. V. Lowry, J. R. Lead, E. Viparelli and M. Baalousha (2015). "Modeling nanomaterial environmental fate in aquatic systems." Environmental science & technology **49**(5): 2587-2593.

Diegoli, S., A. L. Manciulea, S. Begum, I. P. Jones, J. R. Lead and J. A. Preece (2008). "Interaction between manufactured gold nanoparticles and naturally occurring organic macromolecules." Science of the Total Environment **402**(1): 51-61.

Fabrega, J., S. N. Luoma, C. R. Tyler, T. S. Galloway and J. R. Lead (2011). "Silver nanoparticles: behaviour and effects in the aquatic environment." Environment international **37**(2): 517-531.

Fick, A. (1855). "Ueber diffusion." Annalen der Physik **170**(1): 59-86.

Gorban, A., H. Sargsyan and H. Wahab (2011). "Quasichemical models of multicomponent nonlinear diffusion." Mathematical Modelling of Natural Phenomena **6**(05): 184-262.

Gottschalk, F., T. Sun and B. Nowack (2013). "Environmental concentrations of engineered nanomaterials: review of modeling and analytical studies." Environmental Pollution **181**: 287-300.

Ha, H. and J. Payer (2011). "The effect of silver chloride formation on the kinetics of silver dissolution in chloride solution." Electrochimica acta **56**(7): 2781-2791.
Hendricks, D. W. (2006). Water treatment unit processes: physical and chemical, CRC press.
Hinderliter, P. M., K. R. Minard, G. Orr, W. B. Chrisler, B. D. Thrall, J. G. Pounds and J. G. Teeguarden (2010). "ISDD: a computational model of particle sedimentation, diffusion and target cell dosimetry for in vitro toxicity studies." Particle and fibre toxicology **7**(1): 36.
Hitchman, A., G. H. S. Smith, Y. Ju-Nam, M. Sterling and J. R. Lead (2013). "The effect of environmentally relevant conditions on PVP stabilised gold nanoparticles." Chemosphere **90**(2): 410-416.
Hotze, E. M., T. Phenrat and G. V. Lowry (2010). "Nanoparticle aggregation: challenges to understanding transport and reactivity in the environment." Journal of environmental quality **39**(6): 1909-1924.
Huynh, K. A. and K. L. Chen (2011). "Aggregation kinetics of citrate and polyvinylpyrrolidone coated silver nanoparticles in monovalent and divalent electrolyte solutions." Environmental science & technology **45**(13): 5564-5571.
Ju-Nam, Y. and J. R. Lead (2008). "Manufactured nanoparticles: an overview of their chemistry, interactions and potential environmental implications." Science of the total environment **400**(1): 396-414.
Kvitek, L., A. Panáček, J. Soukupova, M. Kolar, R. Vecerova, R. Prucek, M. Holecová and R. Zboril (2008). "Effect of surfactants and polymers on stability and antibacterial activity of silver nanoparticles (NPs)." The Journal of Physical Chemistry C **112**(15): 5825-5834.
La Farre, M., S. Pérez, L. Kantiani and D. Barceló (2008). "Fate and toxicity of emerging pollutants, their metabolites and transformation products in the aquatic environment." TrAC Trends in Analytical Chemistry **27**(11): 991-1007.
Levard, C., E. M. Hotze, G. V. Lowry and G. E. Brown Jr (2012). "Environmental transformations of silver nanoparticles: impact on stability and toxicity." Environmental science & technology **46**(13): 6900-6914.
Levard, C., S. Mitra, T. Yang, A. D. Jew, A. R. Badireddy, G. V. Lowry and G. E. Brown Jr (2013). "Effect of chloride on the dissolution rate of silver nanoparticles and toxicity to E. coli." Environmental science & technology **47**(11): 5738-5745.
Levard, C., B. C. Reinsch, F. M. Michel, C. Oumahi, G. V. Lowry and G. E. Brown Jr (2011). "Sulfidation processes of PVP-coated silver nanoparticles in aqueous solution: impact on dissolution rate." Environmental science & technology **45**(12): 5260-5266.
Liu, J. and R. H. Hurt (2010). "Ion release kinetics and particle persistence in aqueous nano-silver colloids." Environmental science & technology **44**(6): 2169-2175.
Lowry, G. V., K. B. Gregory, S. C. Apte and J. R. Lead (2012). "Transformations of nanomaterials in the environment." Environmental science & technology **46**(13): 6893-6899.
Manciulea, A., A. Baker and J. R. Lead (2009). "A fluorescence quenching study of the interaction of Suwannee River fulvic acid with iron oxide nanoparticles." Chemosphere **76**(8): 1023-1027.
Navarro, E., A. Baun, R. Behra, N. B. Hartmann, J. Filser, A.-J. Miao, A. Quigg, P. H. Santschi and L. Sigg (2008). "Environmental behavior and ecotoxicity of engineered nanoparticles to algae, plants, and fungi." Ecotoxicology **17**(5): 372-386.
Peijnenburg, W. J., M. Baalousha, J. Chen, Q. Chaudry, F. Von Der Kammer, T. A. Kuhlbusch, J. Lead, C. Nickel, J. T. Quik and M. Renker (2015). "A review of the properties and processes determining the fate of engineered nanomaterials in the aquatic environment." Critical Reviews in Environmental Science and Technology(just-accepted): 00-00.
Piccinno, F., F. Gottschalk, S. Seeger and B. Nowack (2012). "Industrial production quantities and uses of ten engineered nanomaterials in Europe and the world." Journal of Nanoparticle Research **14**(9): 1-11.
Quik, J., I. Velzeboer, M. Wouterse, A. Koelmans and D. Van de Meent (2014). "Heteroaggregation and sedimentation rates for nanomaterials in natural waters." Water research **48**: 269-279.
Römer, I., T. A. White, M. Baalousha, K. Chipman, M. R. Viant and J. R. Lead (2011). "Aggregation and dispersion of silver nanoparticles in exposure media for aquatic toxicity tests." Journal of Chromatography A **1218**(27): 4226-4233.
Socolofsky, S. A. and G. H. Jirka (2005). "Special topics in mixing and transport processes in the environment." Engineering—lectures, fifth ed., Coastal and Ocean Engineering Division, Texas A&M University.
Tejamaya, M., I. Römer, R. C. Merrifield and J. R. Lead (2012). "Stability of citrate, PVP, and PEG coated silver nanoparticles in ecotoxicology media." Environmental science & technology **46**(13): 7011-7017.
Thurman, E. M. (2012). Organic geochemistry of natural waters, Springer Science & Business Media.
United States Environmental Protection Agency USA EPA, (2002), "Methods for Measuring the Acute Toxicity of Effluents and Receiving Waters to Freshwater and Marine Organisms", Fifth Edition, **EPA-821-R-02-012**

United States Environmental Protection Agency USA EPA (2009)."Method 415.3: "Determination of Total Organic Carbon and Specific UV Absorbance at 254 nm in Source Water and Drinking Water." Revision 1.2. Document no. **EPA/600/R-09/122.**

Zhang, H., J. A. Smith and V. Oyanedel-Craver (2012). "The effect of natural water conditions on the anti-bacterial performance and stability of silver nanoparticles capped with different polymers." Water research **46**(3): 691-699.

Zook, J. M., S. E. Long, D. Cleveland, C. L. A. Geronimo and R. I. MacCuspie (2011). "Measuring silver nanoparticle dissolution in complex biological and environmental matrices using UV–visible absorbance." Analytical and bioanalytical chemistry **401**(6): 1993-2002.